LONG-TERM ORBIT PREDICTION OF HIGH-ALTITUDE EARTH SATELLITES

C Ulivieri & A Agneni

Università degli Studi di Roma "La Sapienza", Dipartimento Aerospaziale
Via Eudossiana, 18 - 00184 Roma (Italy)

ABSTRACT

The paper presents the results of an investigation into the long-period evolution of the orbital plane of uncontrolled high-altitude Earth satellites, under the luni-solar gravitational effects, which can be independently treated with a good approximation from the other long-term perturbative effects. Since the computer programs, usually employed for orbit prediction during the satellite operational life, result very time-consuming it was previously developed a semi-analytical model for geostationary orbits, that, beside of the noticeable computer time reduction, provides sufficient accuracy over very long periods. The model has been extended to any orbital inclination for high altitude satellites; in particular, orbits highly affected by the motion of the lunar orbital plane have been investigated.

Keywords: luni-solar perturbations, circular orbits, long-term orbit prediction.

1. INTRODUCTION

The perturbations acting on the orbital plane of relatively distant satellites (altitude greater than two Earth radii), due to the gravitational attractions of the Sun and Moon, become comparable to that one due to the Earth oblateness. Then the satellite pole moves from its initial position according to:

i) two short-term periodic evolutions caused by the different temporal orientation of the satellite orbital plane with respect to the distant perturbing body positions; the corresponding periods are about one half of the evolution time of the perturbing body relative motion with respect to the Earth. For 24-hour satellites the maximum amplitude in inclination is about 0.025 deg for the solar effect, while values around 0.0035 deg are found for the lunar one (Ref. 1);

ii) a long-term "periodic" motion with periods from 5 to about 400 years depending on the satellite altitude and on the initial conditions of the orbital pole. For no longer controlled geostationary satellites a period of about 53 years and a maximum inclination of about 15 deg are found.

While the short-term evolution can be evaluated by an accurate numerical integration of the equations of motion, the long-term evolution of the orbital plane has been faced by approximated approaches, which allow a significant computer time reduction. Although most of them are oriented to geostationary orbits and valid for small inclinations ($i < 18°$) (Refs. 2-5), general but qualitative results can be obtained in closed form if the lunar orbital pole is assumed coincident with the ecliptic one (Ref. 6).

A geometrical model, including the effect of the lunar plane motion, has been developed by the authors in a previous work for predicting the long-term evolution of geosynchronous orbits (Ref. 7). The results have shown a satisfactory agreement with corresponding orbital predictions obtained by accurate numerical computations. This simplified model, that averages the disturbing functions over the mean anomalies of the satellite and of the perturbing bodies, does not take into account other long-term perturbative effects, such as the solar radiation pressure and the higher terms of terrestrial gravitational field, which significantly affect the pole motion only after a few decades. On the other hand the disturbing function includes the n lower term of the gravitational attractions of the Sun ($n = 3$) and the Moon ($n = 6$). With the same assumptions, the long-term orbital pole evolution of distant circular orbits for any initial conditions has been investigated in this paper; in particular, the trajectories highly affected by the lunar plane motion have been considered.

The results, whose accuracy has been verified by accurate numerical predictions, show significant differences from the trajectories obtained by means of methods considering a fixed geometry.

Proceedings of the Second International Symposium on Spacecraft Flight Dynamics, Darmstadt, FR Germany, 20–23 October 1986 (ESA SP-255, Dec. 1986)

2. THE ORBITAL POLE EVOLUTION

2.1 Geometrical considerations

With the aforesaid assumptions, the long-term motion of the satellite orbital pole ($\vec{K}$) is described, in an inertial frame, by the vectorial equation, only valid for circular orbits:

$$\dot{\vec{K}} = \vec{K} \times \vec{R} \qquad (1)$$

where $\vec{R}$ is the resultant of regressions around three axes corresponding to the solar and lunar orbital poles and to the terrestrial polar axis. Whereas the ecliptic pole can be considered fixed, the Moon orbital pole is regressing around the ecliptic one with a period of 18.61 years at a constant inclination of 5.145 deg.

For short-time intervals, the lunar orbital pole can be assumed in a time-averaged fixed position and then the simultaneous precessions are performed around fixed axes and the differential equations of motion can be solved in closed form. Two prime integrals can be found: the first giving the known condition that the magnitude of the satellite angular momentum is a constant (which reduces to unity with a suitable normalization), while the second one implies that the disturbing function is a constant of the motion (λ_0). This latter condition, referred to an inertial rectangular frame represents a quadric surface, which is generally an ellipsoid but becomes an elliptic cylinder when the three regression poles are coplanar. For any fixed position of the lunar pole, $\vec{K}$ moves on a spherical ellipse, intersection of the ellipsoid (or elliptic cylinder) with the unit sphere, and its temporal evolution is given by an elliptic integral of the first kind.

As a consequence of the lunar plane regression, the intersection is time-varying and the motion of the satellite orbital pole, starting from the initial conditions, can be faced by means of a step-by-step procedure (Ref. 7).

The principal axes of the quadric surface (ξ, η, ζ) move, with the same period of the lunar pole motion, around three directions corresponding to the principal axes (x, y, z) of the elliptic cylinder obtained when the lunar plane is assumed coincident with the ecliptic. While y is always coincident with the Vernal axis, the directions of the other two axes (the rectangular frame being right-handed) are determined by the angle δ measured counterclockwise from the terrestrial polar axis; δ increases with the satellite altitude (h), going from almost zero for $h = 2R_\oplus$ to about 18 deg at $h = 9R_\oplus$ (being $R_\oplus$ the Earth's radius) (Fig. 1).

If the eigenvalues of the matrix associated to the quadric surface are considered in increasing order $\lambda_1 < \lambda_2 < \lambda_3$, the pole $\vec{K}$ will performe a long-term trajectory encircling the z axis if $\lambda_2 < \lambda_0 \leq \lambda_3$, or y axis if $\lambda_1 \leq \lambda_0 < \lambda_2$; on the contrary no trajectories are performed around the x axis ($\lambda_0 = \lambda_2$).

The two allowable families of trajectories are separated by the circles deriving from the intersections of the unit sphere with "limit" planes, whose common straight line is the ξ axis and whose inclination with respect to the $\xi\eta$ plane is α (Fig. 2), varying also with the satellite altitude (Fig. 1).

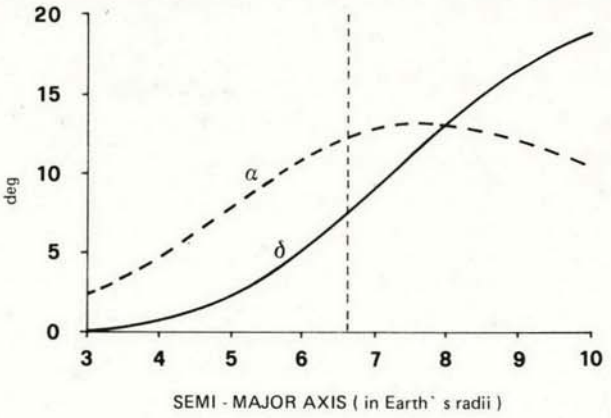

Fig. 1 - The inclinations, δ, of the x-y plane with respect to the equatorial one, and α, of the "limit" planes with respect to the ξ-η plane as functions of the orbital semi-major axis (in Earth radii). The dashed vertical line is relative to the 24-hour orbit.

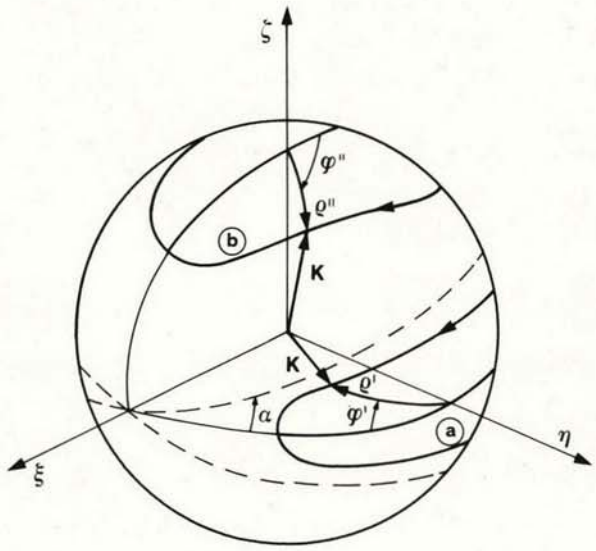

Fig. 2. Trajectories of the satellite orbital pole on the unit sphere relative to a generic position of the lunar orbital plane: (a) $\lambda_0 < \lambda_2$; (b) $\lambda_0 > \lambda_2$.

2.2 Temporal evolution

The quadric surface equation written in its canonical form is

$$\lambda_2 \xi^2 + \lambda_1 \eta^2 + \lambda_3 \zeta^2 = \lambda_0 \qquad (2)$$

however the position of the satellite pole on the performed trajectory, for the sake of convenience, is determined by the two polar coordinates: the arc-length from the axis around which the pole is moving (η or ζ) and the dihedral angle measured from the plane on which the semi-major axis of the spherical ellipse lies (Fig. 2). The sphero-conic, intersection of the quadric with the unit sphere, can so be written

$$\frac{\sin^2\rho \cos^2\varphi}{A^2} + \frac{\sin^2\rho \sin^2\varphi}{B^2} = 1 \qquad (3)$$

where the coordinates (ρ,φ) and the semiaxes (A,B) are expressed in Table 1 for the two cases respectively. For any fixed position of the principal axes, the temporal evolution of $\vec{K}$ on the sphero-conic is described by the equation

$$\frac{d}{dt}(\cos\rho) = -\frac{\partial\lambda_0}{\partial\varphi} \qquad (4)$$

which becomes

$$H dt = \frac{d\mu}{\sqrt{1 - k^2 \sin^2\mu}} \qquad (5)$$

after introducing an auxiliary angle μ defined by

$$\begin{cases} \sin\mu = \dfrac{\sin\rho \cos\varphi}{A} \\ \cos\mu = \dfrac{\sin\rho \sin\varphi}{B} \end{cases} \qquad (6)$$

The expressions assumed by the angular velocity H and by the modulus k are shown in Table 1.

In order to solve the elliptic integral of the first kind (5) for any value of k ($0 \leq k < 1$ according to the initial position of the pole $\vec{K}$), the Landen transformation and the Gauss limit, linked with arithmetic and geometric means, have been used (Ref. 8).

3. EXAMPLES OF $\vec{K}$ EVOLUTIONS

The lunar plane motion can remarkably influence the long-term orbital plane evolution of high altitude satellites; the results, obtained either when the lunar pole is assumed coincident with the ecliptic one or when the effect due to the motion of the lunar pole is considered small, do not turn out to be acceptable for any initial condition and satellite altitude. The use of the geometrical model allows instead to predict the satellite pole evolution with a sufficient accuracy.

The lunar pole regression around the ecliptic influences the trajectories of $\vec{K}$, expecially when the initial conditions are close to the evolutions of the η and ζ axes. Whereas ζ, inclined of an angle γ with respect to z, performes almost circular trajectories on the unit sphere, η evolves as in Fig. 3. Table 2 shows, for several orbital semi-major axes (in Earth radii), the corresponding values of δ, of the maximum amplitude (ε_{max}) assumed by η with respect to y and of the mean value of γ ($\bar{\gamma}$).

For 24-hour orbits ($r/R_\oplus = 6.6$), typical evolutions of $\vec{K}$ have been considered with different initial conditions. Figures 3 and 4 represent two evolutions around the y axis; the effect due to the lunar plane motion appears significant even when the initial position of the satellite orbital pole ($\vec{K}_0$) is rather distant from the trajectory of η (Fig. 3). This stems from the large values assumed by ε.

Table 1.

	η axis	ζ axis
A	$\left[\frac{\lambda_0 - \lambda_1}{\lambda_2 - \lambda_1}\right]^{1/2}$	$\left[\frac{\lambda_3 - \lambda_0}{\lambda_3 - \lambda_2}\right]^{1/2}$
B	$\left[\frac{\lambda_0 - \lambda_1}{\lambda_3 - \lambda_1}\right]^{1/2}$	$\left[\frac{\lambda_3 - \lambda_0}{\lambda_3 - \lambda_1}\right]^{1/2}$
H	$[(\lambda_3 - \lambda_0)(\lambda_2 - \lambda_1)]^{1/2}$	$-[(\lambda_0 - \lambda_1)(\lambda_3 - \lambda_2)]^{1/2}$
k	$\left[\frac{(\lambda_3 - \lambda_2)(\lambda_0 - \lambda_1)}{(\lambda_3 - \lambda_0)(\lambda_2 - \lambda_1)}\right]^{1/2}$	$\left[\frac{(\lambda_3 - \lambda_0)(\lambda_2 - \lambda_1)}{(\lambda_0 - \lambda_1)(\lambda_3 - \lambda_2)}\right]^{1/2}$
ρ	ρ'	ρ''
φ	φ'	φ''

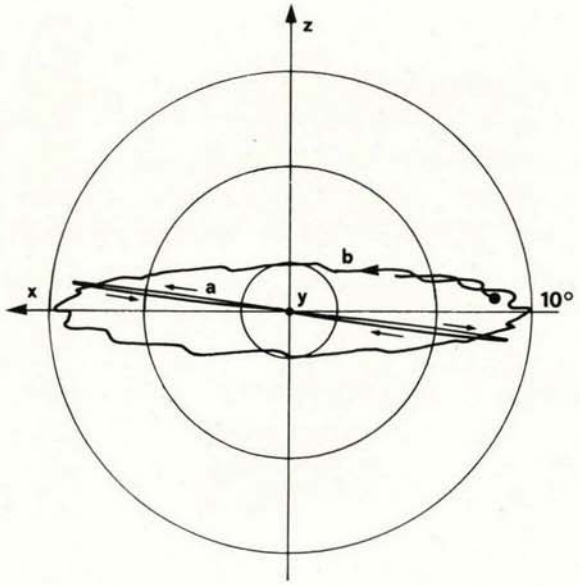

Fig. 3 - a) - Time evolution of the η axis around y on the unit sphere; its inclination on the plane x-y is almost δ;
b) - 200 year evolution of a 24-hour satellite orbital pole, whose initial conditions are: i_0 = 88.3 deg, Ω_0 = 98.2 deg and epoch Jan. 1985.

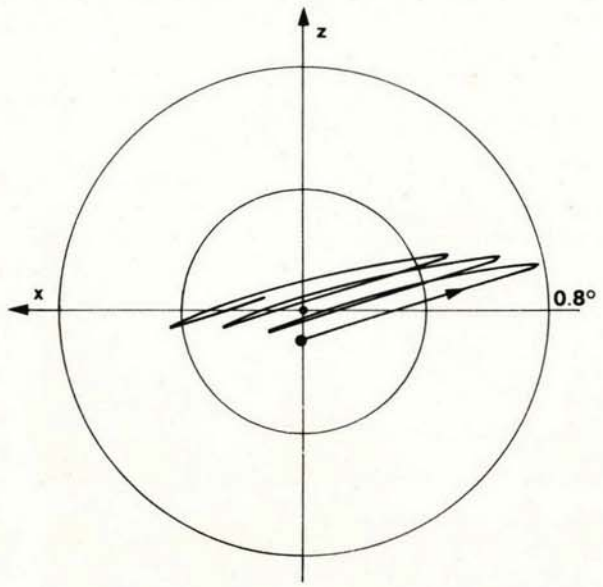

Fig. 4 - Evolution of a 24-hour satellite pole, whose initial conditions are: i_0 = 90.1 deg, Ω_0 = 90 deg and epoch March 1969.

Table 2.

$r/R_\oplus$	δ (deg)	ε_{max} (deg)	$\bar{\gamma}$ (deg)
3.0	0.19	8.939	0.026
4.5	1.47	8.942	0.204
6.6	7.40	8.961	1.092
10.0	18.83	9.298	2.892

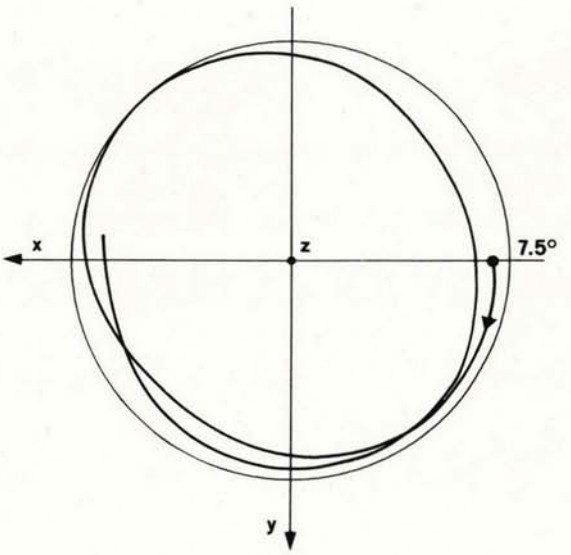

Fig. 5 - Time evolution of $\vec{K}$ for a geostationary satellite:
i_0 = 0.33 deg, Ω_0 = 94.1 deg and epoch July 1983.

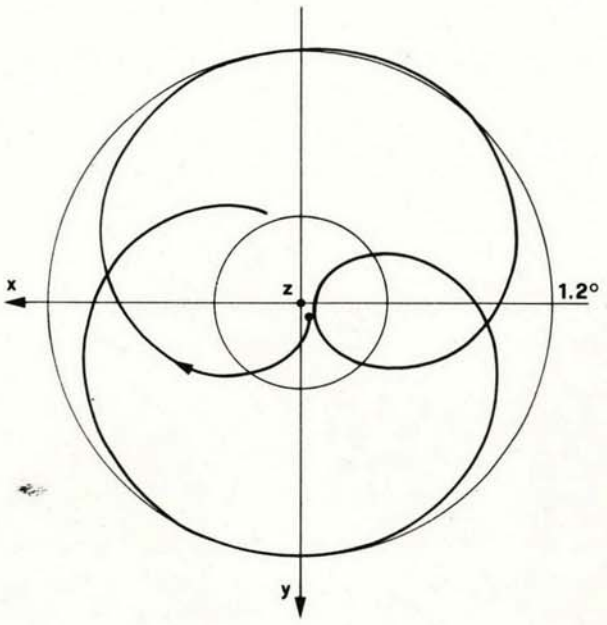

Fig. 6 - Time evolution of $\vec{K}$ for a 24-hour satellite with the following initial conditions:
i_0 = 7.4 deg, Ω_0 = 0.5 deg and epoch Jan. 1969.

On the contrary, the small values of γ and the almost circular trajectories of ζ make $\vec{K}$ perform smoother evolutions, which are rather similar to spherical ellipses when the initial position of the satellite orbital pole is far enough from z (Fig. 5). When $\vec{K}_0$ is close to the ζ trajectory (in particular in Fig. 6 $\vec{K}_0$ is inside it) the $\vec{K}$ evolutions become strongly deformed.

For semi-major axes different from 24-hour orbits the evolution of $\vec{K}$ is similar; Figure 7 shows the evolution for $r/R_\oplus = 10$ and $\vec{K}_0$ located inside the ζ trajectory.

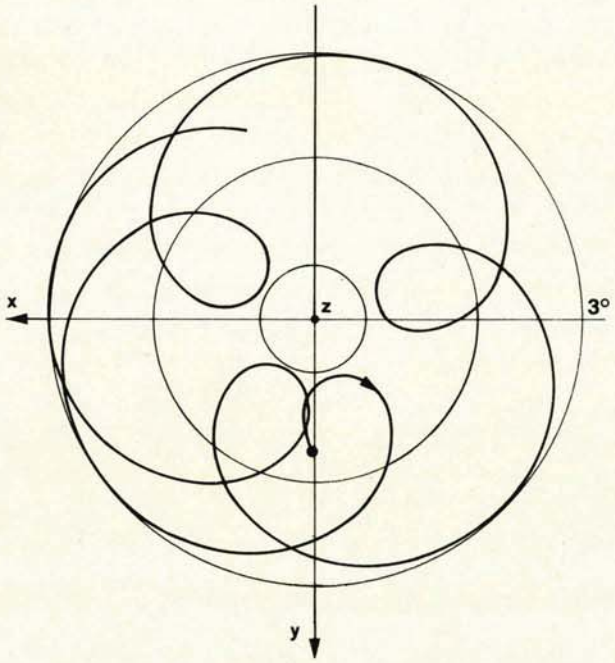

Fig. 7 - Temporal evolution of $\vec{K}$ for the conditions: $i_0 = 18.89$ deg, $\Omega_0 = 4.55$ deg and epoch Apr. 1978.

A different behaviour has been found when the angular velocity H becomes almost equal to the lunar pole regression rate (19.34 deg/year). This happens, for example, if the satellite is placed at $r/R_\oplus \cong 4.54$. Figures 8 and 9 represent the $\vec{K}$ evolutions for two different initial conditions; one can see that, after an initial approach to z axis due to the relative initial positions of $\vec{K}$ and ζ, in the long run the satellite orbital pole assumes a spiral-shaped trajectory. Because of the small value of $\bar{\gamma}$, almost circular evolutions have been found for initial conditions distant from z.

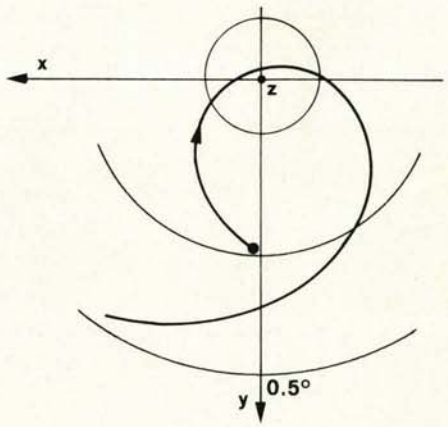

Fig. 8 - Temporal evolution of the orbital pole for the initial conditions: $i_0 = 1.5$ deg, $\Omega_0 = 11.01$ deg and epoch Apr. 1978.

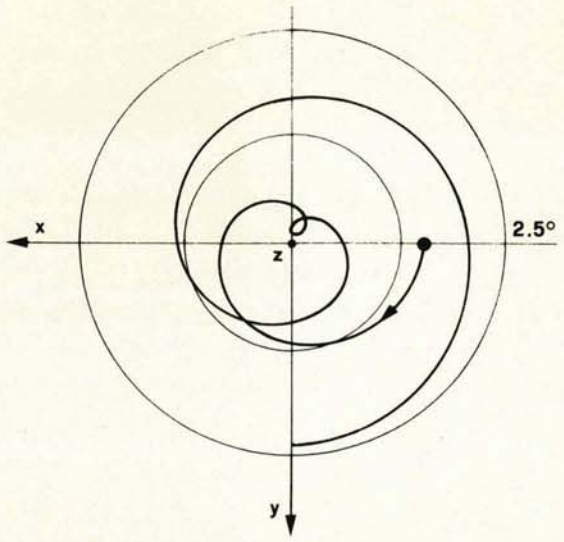

Fig. 9 - Temporal evolution of $\vec{K}$ for the initial conditions: $i_0 = 0.1$ deg, $\Omega_0 = 0.1$ deg and epoch Jan. 1974.

The long-term orbit predictions, obtained with the geometrical model, have been compared with the results of a propagator, which numerically integrates the equations of motion, over almost two decades. The comparison, made for evolutions highly affected by the lunar plane regression (cases in Figs. 3, 8 and 9), has shown a satisfactory agreement as for the geostationary orbits.

4. ACKNOWLEDGEMENTS

This work was supported by CNUCE, Institute of the Italian National Research Council. The authors are also grateful to the components of the Space Group of the same Institute for their assistance during the accomplishment of the paper.

5. REFERENCES

1. C.N.E.S. 1983, Le mouvement du satellite, Toulouse, Cepadues Ed., 578-587.

2. Kamel A and Tibbitts R 1973, Some useful results on initial node locations for near-equatorial circular satellite orbits, *Celestial Mechanics Journal* 8 (1), 45-73.

3. Graf O F Jr 1975, Lunar and solar perturbations on the orbit of a geosynchronous satellite, *AAS/AIAA Astrodynamics Specialist Conference*, Nassau 28-30 July 1975.

4. Richardson D L 1976, The long-period motion of 24-hour satellites, *AIAA/AAS Astrodynamics Conference*, San Diego 18-20 August 1976.

5. Van der Ha J C 1986, Long-term evolution of near-geostationary orbits, *J. of Guidance Control and Dynamics* 9 (3), 363-370.

6. Allan R R and Cook G E 1964, The long-period motion of the plane of a distant circular orbit, *Proceedings of the Royal Society* 280A, 97-109.

7. Agneni A et al. 1986, A geometrical model for predicting the long-term Luni-Solar effects on geosynchronous satellites, *J. Astronautical Sciences*, 34 (3).

8. Tricomi F G 1932, *Funzioni ellittiche*, Bologna, Zanichelli 184-261.